An Organic-inorganic Hybrid Two-dimensional Bilayer Assembled from 1:2-Type $[Er(\alpha\text{-}PW_{11}O_{39})_2]^{11-}$ Moieties and $[Cu(dap)_2]^{2+}$ Linkers①

LUO Jie SONG Kai-Fang ZHAO Hao-Zhe
ZHAO Jun-Wei CHEN Li-Juan②
(*Henan Key Laboratory of Polyoxometalate Chemistry*, *Institute of Molecular and Crystal Engineering, College of Chemistry and Chemical Engineering, Henan University, Kaifeng* 475004, *China*)

ABSTRACT A new organic-inorganic hybrid phosphotungstate-based Cu^{II}–Er^{III} heterometallic derivative $[Cu(dap)_2(H_2O)][Cu(dap)_2]_{4.5}[Er(\alpha\text{-}PW_{11}O_{39})_2]\cdot 4H_2O$ (**1**, dap = 1,2-diaminopropane) has been hydrothermally prepared and characterized by elemental analysis, IR spectra and X-ray single-crystal diffraction. **1** belongs to the triclinic space group $P\bar{1}$ with a = 13.453(3), b = 20.137(4), c = 24.565(4) Å, α = 103.468(4), β = 103.829(4), γ = 98.296(4)°, V = 6148.0(19) Å^3, Z = 2, μ = 22.212 mm^{-1}, $GOOF$ = 1.030, R = 0.0744 and wR = 0.1700. Structural analysis indicates that **1** exhibits a special two-dimensional double-layer structure constructed from 1:2-type $[Er(\alpha\text{-}PW_{11}O_{39})_2]^{11-}$ moieties and $[Cu(dap)_2]^{2+}$ linkers. From the topological viewpoint, **1** displays a scare two-dimensional five-connected topology in which the $[Er(\alpha\text{-}PW_{11}O_{39})_2]^{11-}$ moieties function as the five-connected nodes. Furthermore, its thermogravimetric behavior has been studied.

Keywords: polyoxometalate, heterometallic complex, phosphotungstate,
DOI:10.14102/j.cnki.0254-5861.2011-0817

1 INTRODUCTION

Designed synthesis and exploitation of novel organic-inorganic hybrid materials based on metal ions, inorganic building blocks and multifunctional organic ligands under suitable conditions have attracted considerable attention because of not only their remarkable structures and properties but also their potential applications in the areas of catalysis, medicine, magnetism, luminescence and materials science[1–4]. It is well-known that polyoxometalates (POMs) are versatile inorganic building blocks for constructing molecule-based materials by means of their rich and active surface oxygen atoms. Among them, lacunary Keggin-type phosphotungstate (PT) precursors can often act as useful inorganic polydentate ligands to incorporate transition-metal (TM) or lanthanide (Ln) cations, manufacturing TM-substituted PTs (TMSPTs) or Ln-substituted PTs (LSPTs)[5–11]. In the past several years, exploring and discovering novel TM–Ln heterometallic Keggin-type PTs (TLHKPs) have gradually become an important research branch in the POM chemistry and some TLHKPs have been reported. For example, in 2008, Liu et al communicated a class of 1-D TLHKPs $[\{Ln(PW_{11}O_{39})_2\}\{Cu_2(bpy)_2(\mu\text{-ox})\}]^{9-}$ (Ln

Received 22 May 2015; accepted 22 July 2015 (**CCDC 1401461**)
① This work was supported by the Natural Science Foundation of China (21301049, U1304208), and the Natural Science Foundation of Henan Province (122300410106)
② Corresponding author. E-mails: ljchen@henu.edu.cn and zhaojunwei@henu.edu.cn

= La^{III}, Pr^{III}, Eu^{III}, Gd^{III}, Yb^{III}) based on bis(undecatungstophosphate)lanthanates and dinuclear copper(II)-oxalate complexes[12]. In 2011, Niu et al discovered a family of unique organic-inorganic hybrid TLHKPs with mixed en and 2,2′-bipy ligands $\{[Cu(en)_2]_{1.5}[Cu(en)(2,2'\text{-bipy})(H_2O)_n]Ln[(\alpha\text{-}PW_{11}O_{39})_2]\}^{6-}$ (Ln = Ce^{III}, Pr^{III})[13] $\{[Cu(en)_2]_2(H_2O)[Cu(en)(2,2'\text{-bipy})]Ln[(\alpha\text{-}HPW_{11}O_{39})_2]\}^{4-}$ (Ln = Gd^{III}, Tb^{III}, Er^{III})[13] and $\{[Cu(en)_2]_{1.5}[Cu(en)(2,2'\text{-bipy})]Nd[(\alpha\text{-}H_5PW_{11}O_{39})_2]\}^{3-}$[13]. In 2013, Yang's group synthesized two novel oxalate-bridging TLHKPs $[Cu(en)_2(H_2O)][Cu(en)_2][Tb(\alpha\text{-}PW_{11}O_{39})(H_2O)_2(ox)Cu(en)]\cdot 6H_2O$[14] and $\{[Cu(en)_2(H_2O)]_4[Sm(\alpha\text{-}PW_{11}O_{39})(CH_3COO)(H_2O)]_2\}^{2-}$[15]. Recently, during the course of our investigating the reactions of lacunary Keggin-type POM precursors with TM and Ln mixed cations in the participation of organic groups[16-19], we obtained an organic-inorganic hybrid PT-based Cu–Er heterometallic derivative $[Cu(dap)_2(H_2O)][Cu(dap)_2]_{4.5}[Er(\alpha\text{-}PW_{11}O_{39})_2]\cdot 4H_2O$(**1**) by the hydrothermal reaction of $Na_9[A\text{-}\alpha\text{-}PW_9O_{34}]\cdot 7H_2O$, $CuCl_2\cdot 2H_2O$, $ErCl_3$ and dap. X-ray diffraction analysis indicates that **1** displays a rare 2-D sheet motif built by 1:2-type $[Er(\alpha\text{-}PW_{11}\text{-}O_{39})_2]^{11-}$ subunits and $[Cu(dap)_2]^{2+}$ bridges.

2 EXPERIMENTAL

2. 1 Apparatus and materials

$Na_9[A\text{-}\alpha\text{-}PW_9O_{34}]\cdot 7H_2O$ was synthesized according to the previous method[20] and identified by IR spectra. Other chemicals were obtained from commercial resources and used without further purification. C, H, and N analyses were carried on a Perkin-Elmer 240C elemental analyzer. IR data were collected on a Nicolet170 SXFT-IR spectrometer using a sample powder palletized with KBr in the range of 4000～400 cm^{-1}. The thermogravimetric (TG) analysis was performed on Perkin-Elmer 7 analyzer in N_2 atmosphere at a heating rate of 10 ^oC/min from 25 to 1000 ^oC.

2. 2 Synthesis of 1

$Na_9[A\text{-}\alpha\text{-}PW_9O_{34}]\cdot 7H_2O$ (0.246 g, 0.096 mmol), $CuCl_2\cdot 2H_2O$ (0.063 g, 0.370 mmol), $ErCl_3$ (0.042 g, 0.153 mmol) and dap (0.05 mL, 0.579 mmol) were successively suspended in H_2O (5 mL, 278 mmol). The resulting mixture was stirred for 2 h, sealed in a 25 mL Teflon-lined stainless-steel autoclave, kept at 160 ^oC for 5 days, and then slowly cooled to room temperature. Purple block crystals were collected by filtering, washed with distilled water and dried in air. Yield: *ca.* 30% (based on $Na_9[A\text{-}\alpha\text{-}PW_9O_{34}]\cdot 7H_2O$). Anal. Calcd. (%) for $C_{33}H_{120}Cu_{5.50}ErN_{22}O_{83}P_2W_{22}$: C, 5.85; H, 1.78; N, 4.55%. Found: C, 5.86; H, 1.76; N, 4.53%.

2. 3 X-ray crystallography

Diffraction intensity data of **1** were collected on a Bruker APEX-II CCD detector at 296(2) K with Mo$K\alpha$ radiation (λ = 0.71073 Å) using a multi-scan mode in the range of $1.56 \leqslant \theta \leqslant 25.00°$ and corrected for Lorentz and polarization effects as well as SADABS program. Its structure was solved by direct methods using the SHELXS-97 program[21] and refined by full-matrix least-squares method on F^2 using the SHELXL-97 program[22]. All non-H atoms except for some C, N and water O atoms were refined anisotropically. All H atoms were placed in idealized positions and refined with a riding model using default SHELXL parameters. Those H atoms attached to lattice water molecules were not located. The final R = 0.0744, wR = 0.1700 ($w = 1/[\sigma^2(F_o^2) + (0.0508P)^2 + 0.0000P]$, $P = (F_o^2 + 2F_c^2)/3$), S = 1.030, $(\Delta/\sigma)_{max}$ = 0.002, $(\Delta\rho)_{max}$ = 4.654 and $(\Delta\rho)_{min}$ = –4.697 e/Å^3. Selected bond lengths and bond angles are displayed in Table 1.

3 RESULTS AND DISCUSSION

3. 1 Structural description

Single-crystal X-ray diffraction reveals that **1** belongs to the triclinic space group $P\bar{1}$ and displays a peculiar 2-D double sheet structure established by 1:2-type $[Er(\alpha\text{-}PW_{11}O_{39})_2]^{11-}$ moieties through $[Cu(dap)_2]^{2+}$ connectors. The molecular structural unit of **1** (Fig. 1a) contains 1 classical 1:2-type $[Er(\alpha\text{-}PW_{11}O_{39})_2]^{11-}$ moiety, 1 $[Cu(dap)_2(H_2O)]^{2+}$ cation,

4.5 $[Cu(dap)_2]^{2+}$ cations and 4 water molecules of crystallization. It should be pointed out that the 1:2-type $[Er(\alpha\text{-}PW_{11}O_{39})_2]^{11-}$ moiety (Fig. 1b) is composed of two monovacant Keggin $[\alpha\text{-}PW_{11}O_{39}]^{7-}$ fragments bridged by a Er^{3+} ion, leading to a typical sandwich-type bis(undecatungstophosphate) lanthanate structure. As a matter of fact, this 1:2 type bis(undecatungstophosphate)lanthanate $[Ln^{III/IV}(\alpha\text{-}PW_{11}O_{39})_2]^{n-}$ (Ln^{III}, n = 11; Ln^{IV}, n = 10) was for the first time discovered by Peacock and Weakley in 1971[22, 24]. Furthermore, similar bis(undecamolybdophosphate)lanthanates $[Ln^{III}(\alpha\text{-}PMo_{11}O_{39})_2]^{11-}$ (Ln = trivalent lanthanide cations) were also reported by May and co-workers[25, 26]. From the viewpoint of structural chemistry, there exist 6 crystallographically dependent Cu^{2+} ions in the molecular structural unit in **1**. It should be noted that the $Cu5^{2+}$ ion is situated on the special position with the site occupancy of 0.5, whereas the remaining Cu^{2+} ions occupy the usual sites with the site occupancy of 1 for each. Both $[Cu(1)(dap)_2]^{2+}$ and $[Cu(6)(dap)_2]^{2+}$ supporting ions are embedded in the square pyramidal configuration (Fig. 1c), in which nitrogen atoms from two dap groups (Cu–N: 1.883(3)～2.141(4) Å) occupy the basal plane and a terminal oxygen atom from the $[Er(\alpha\text{-}PW_{11}O_{39})_2]^{11-}$ subunit (Cu–O: 2.311(17)～2.930(20) Å) is located on the conical point. The $[Cu(3)(dap)_2(H_2O)]^{2+}$ pendent ion shows the octahedral geometry (Fig. 1d) constructed from four nitrogen atoms from two dap groups, creating the equatorial plane (Cu–N: 1.988(5)～2.065(5) Å) and an aqueous oxygen atom (Cu–O 2.885(34) Å) together with a terminal oxygen atom from the $[Er(\alpha\text{-}PW_{11}O_{39})_2]^{11-}$ subunit (Cu–O: 2.428(17) Å) sitting on two axial sites. The elongated octahedral environments (Fig. 1d) of $[Cu(2)(dap)_2]^{2+}$, $[Cu(4)(dap)_2]^{2+}$ and $[Cu(5)(dap)_2]^{2+}$ bridging ions are defined by four nitrogen atoms from two dap groups (Cu–N 1.93(3)～2.02(3) Å) and two terminal oxygen atoms from two $[Er(\alpha\text{-}PW_{11}O_{39})_2]^{11-}$ subunits (Cu–O 2.460(15)～2.785(17) Å). The $Er(1)^{3+}$ ion encapsulated in the vacant sites of two $[\alpha\text{-}PW_{11}O_{39}]^{7-}$ fragments illustrates a distorted square antiprism geometry (Fig. 1e), in which four oxygen atoms (O(21), O(24), O(39), O(35)) from one $[\alpha\text{-}PW_{11}O_{39}]^{7-}$ fragment (Er–O: 2.313(16)～2.389(16) Å) form the upper surface of the square antiprism and other four oxygen atoms (O(44), O(47), O(70), O(66)) from the other $[\alpha\text{-}PW_{11}O_{39}]^{7-}$ fragment (Er–O: 2.288(16)～2.402(14) Å) construct the bottom surface of the square antiprism. The standard deviations of the upper and bottom surfaces are 0.0102 and 0.0058 Å, respectively. The distance between the $Er(1)^{3+}$ ion and the upper surface is 1.2691 Å whereas that between the $Er(1)^{3+}$ ion and the bottom surface is 1.2509 Å. The dihedral angle formed by the upper and bottom surfaces is 0.7°. All above-mentioned data manifest that the coordination geometries of the copper and erbium ions are distorted to some extent.

Table 1. Selected Bond Lengths (Å) and Bond Angles (°) for 1

Bond	Dist.	Bond	Dist.	Bond	Dist.	Bond	Dist.
Er(1)–O(47)	2.288(16)	Cu(1)–N(3)	2.06(3)	Cu(3)–N(10)	2.013(5)	Cu(5)–N(17)#3	1.98(2)
Er(1)–O(21)	2.313(16)	Cu(1)–O(38)	2.311(17)	Cu(3)–N(12)	2.065(5)	Cu(5)–N(17)	1.98(2)
Er(1)–O(44)	2.356(16)	Cu(2)–N(5)	1.93(3)	Cu(3)–O(69)	2.428(17)	Cu(5)–N(18)	1.99(2)
Er(1)–O(24)	2.360(14)	Cu(2)–N(7)	1.94(3)	Cu(3)–O(1W)	2.886(4)	Cu(5)–N(18)#3	1.99(2)
Er(1)–O(39)	2.370(14)	Cu(2)–N(8)	1.94(3)	Cu(4)–N(16)	1.98(2)	Cu(5)–O(20)	2.488(3)
Er(1)–O(70)	2.378(13)	Cu(2)–N(6)	1.95(3)	Cu(4)–N(15)	1.98(2)	Cu(5)–O(20) #3	2.488(3)
Er(1)–O(66)	2.402(14)	Cu(2)–O(15)	2.785(4)	Cu(4)–N(14)	1.99(2)	Cu(6)–N(19)	1.883(3)
Cu(1)–N(2)	1.98(3)	Cu(2)–O(78)#1	2.758(4)	Cu(4)–N(13)	2.02(3)	Cu(6)–N(21)	2.025(4)
Cu(1)–N(4)	2.01(3)	Cu(3)–N(11)	1.988(5)	Cu(4)–O(72)	2.460(4)	Cu(6)–N(20)	2.080(4)
Cu(1)–N(1)	2.02(2)	Cu(3)–N(9)	2.010(5)	Cu(4)–O(58) #2	2.580(5)	Cu(6)–N(22)	2.141(4)
Angle	(°)	Angle	(°)	Angle	(°)	Angle	(°)
O(47)–Er(1)–O(21)	77.0(6)	O(21)–Er(1)–O(39)	113.8(5)	O(39)–Er(1)–O(70)	138.4(5)	O(47)–Er(1)–O(66)	115.8(5)
O(47)–Er(1)–O(44)	73.2(6)	O(44)–Er(1)–O(39)	79.6(5)	O(47)–Er(1)–O(35)	139.8(5)	O(21)–Er(1)–O(66)	145.3(5)

To be continued

O(21)–Er(1)–O(44)	139.0(5)	O(24)–Er(1)–O(39)	74.7(5)	O(21)–Er(1)–O(35)	73.5(5)	O(44)–Er(1)–O(66)	74.5(5)
O(47)–Er(1)–O(24)	79.0(5)	O(47)–Er(1)–O(70)	73.4(5)	O(44)–Er(1)–O(35)	144.9(5)	O(24)–Er(1)–O(66)	139.9(5)
O(21)–Er(1)–O(24)	71.9(5)	O(21)–Er(1)–O(70)	80.7(5)	O(24)–Er(1)–O(35)	116.0(5)	O(39)–Er(1)–O(66)	74.6(5)
O(44)–Er(1)–O(24)	75.2(6)	O(44)–Er(1)–O(70)	115.9(5)	O(39)–Er(1)–O(35)	72.5(5)	O(70)–Er(1)–O(66)	73.5(5)
O(47)–Er(1)–O(39)	146.0(5)	O(24)–Er(1)–O(70)	144.7(5)	O(70)–Er(1)–O(35)	75.3(5)	O(35)–Er(1)–O(66)	77.8(5)

Symmetry transformations used to generate the equivalent atoms: #1: *x*, 1+*y*, *z*; #2: –1+*x*, *y*, *z*; #3: 1–*x*, –*y*, 1–*z*

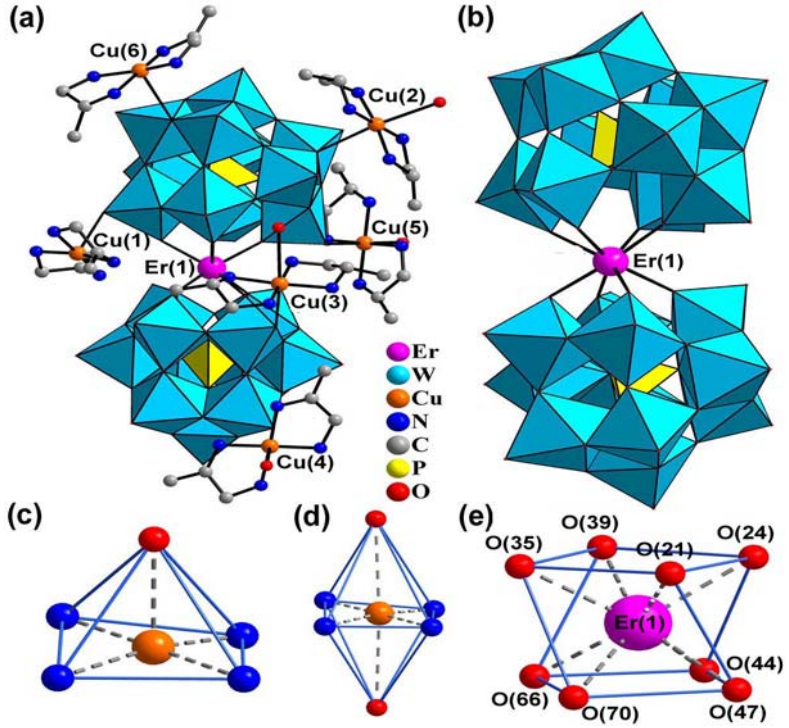

Fig. 1. (a) Structural unit of 1 with selected atom labeling scheme. The protons and lattice water molecules are omitted for clarity. (b) View of the 1:2-type $[Er(\alpha\text{-}PW_{11}O_{39})_2]^{11-}$ moiety. (c) The five-coordinate $\{CuN_4O\}$ square pyramid. (d) The six-coordinate $\{CuN_4O_2\}$ elongated octahedron. (e) The distorted square antiprism geometry of the $Er(1)^{3+}$ ion

More interestingly, each molecular structural unit of **1** is combined with five same ones (Fig. 2a) by means of five $[Cu(dap)_2]^{2+}$ bridges (two $[Cu(2)(dap)_2]^{2+}$, two $[Cu(4)(dap)_2]^{2+}$ and one $[Cu(5)(dap)_2]^{2+}$), giving rise to a unique two-dimensional bilayer structure (Fig. 2b). The most remarkable structural feature is that the two-dimensional bilayer architecture can be viewed as the combination of two neighboring two-dimensional monolayers through the bridging role of $[Cu(5)(dap)_2]^{2+}$ ions (Fig. 3). In order to decrease the steric hindrance, neighboring two monolayers are aligned in the stagger fashion. As far as we know, this two-dimensional bilayer construction mode is very rare in POM chemistry. From the topological viewpoint, the circuit symbols with Schläfli (vertex) notations can be utilized to describe topological structures and facilitate to compare the networks of diverse compositions and metrics[27]. Thus, if each $[Er(\alpha\text{-}PW_{11}O_{39})_2]^{11-}$ moiety can be looked on as a 5-connected node, **1** exhibits a scarce two-dimensional 5-connected topology with short vertex (Schläfli) symbol of $4^8\cdot6^2$ and long topological (O´Keeffe) vertex symbol of $4\cdot4\cdot6_3\cdot4\cdot4\cdot4\cdot6_3\cdot4\cdot4\ 4$ (Fig. 4). It is worth noting that such two-dimensional bilayer **1** with the 5-connected topology is completely different from the three-dimensional Keggin silicotungstate-based TM–Ln heterometallic derivatives $NaH[Cu(dap)_2(H_2O)][Cu(dap)_2]_{4.5}[Ln(\alpha\text{-}SiW_{11}O_{39})_2]\cdot 7H_2O$ ($Ln = Sm^{III}$, Dy^{III}, Gd^{III}) reported by us, which illustrate the 5-connected topology with the Schläfli symbol of $4^6\cdot6^4$ and the O´Keeffe symbol of $6\cdot6\cdot4\cdot4\cdot6\cdot4\cdot4\cdot4\cdot4\ 6_3$[28]. In addition, adjacent bilayer sheets in **1** are arranged in the mode of -AAA-.

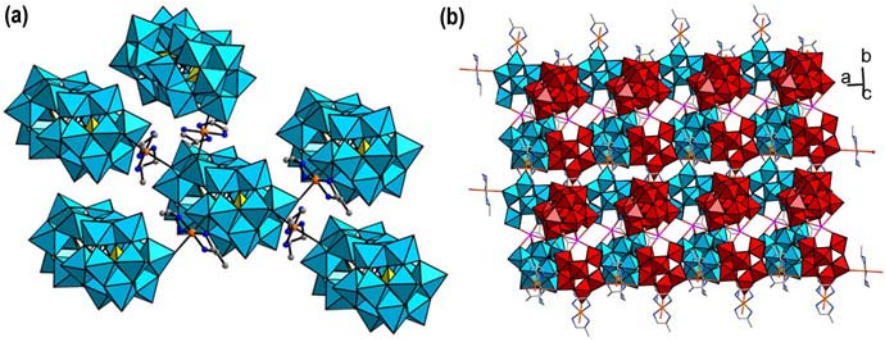

Fig. 2. (a) Combination between a molecular structural unit and five same ones. The $[Cu(1)(dap)_2]^{2+}$ and $[Cu(6)(dap)_2]^{2+}$ supporting ions are omitted for clarity. (b) Top view of the two-dimensional bilayer architecture

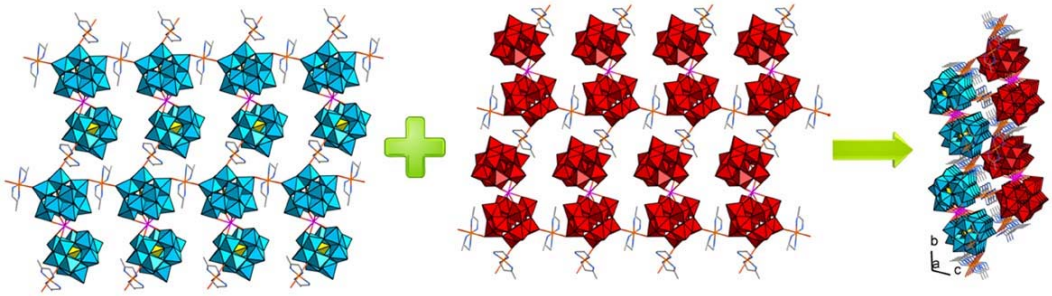

Fig. 3. Schematic combination of two neighboring two-dimensional monolayers through the bridging role of $[Cu(5)(dap)_2]^{2+}$ ions constructing the two-dimensional bilayer architecture

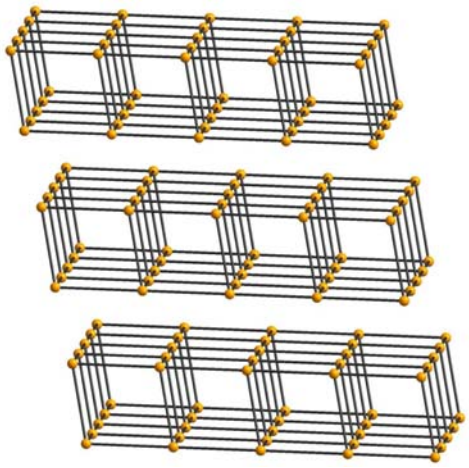

Fig. 4. Topology structure of 1

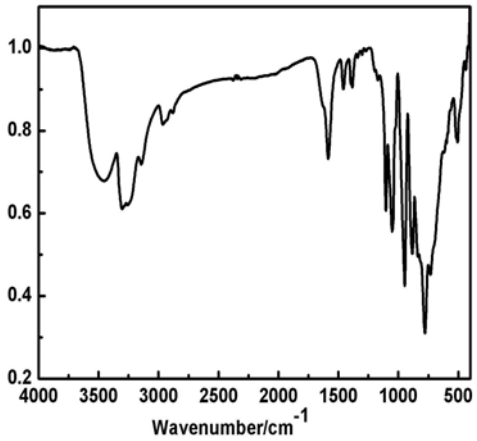

Fig. 5. IR spectrum of 1

3. 2 IR spectrum

In the IR spectrum of **1** (Fig. 5), the characteristic vibration patterns derived from the Keggin-type PT polyoxoanion are observed in the low wavenumber region. Four groups of featured absorption bands centered at 1107, 1049; 945; 879; and 781, 723 cm^{-1} are respectively assigned to the $\nu(P–O_a)$, $\nu(W–O_t)$, $\nu(W–O_b)$ and $\nu(W–O_c)$ vibrations. In comparison with the IR spectrum of α-$Na_7PW_{11}O_{39}\cdot nH_2O$ (1099, 1042; 954; 865; and 809, 728 cm^{-1} for $\nu(P–O_a)$; $\nu(W–O_t)$;$\nu(W–O_b)$ and $\nu(W–O_c)$)[29], the $\nu(W–O_t)$ vibration peak of **1** is somewhat bathochromic, which mainly results from the occurrence of stronger interactions between $[Cu(dap)_2(H_2O)]^{2+}$, $[Cu(dap)_2]^{2+}$ cations and terminal oxygen atoms of $[\alpha$-$PW_{11}O_{39}]^{7-}$ fragments[10]. On the contrary, the $\nu(W–O_b)$ vibration frequency of **1** is hypsochromic, which may be relevant to the insertion of Er^{III} cation to the lacuary positions of two $[\alpha$-$PW_{11}O_{39}]^{7-}$ fragments[29]. Compared with the IR spectrum of $H_3[\alpha$-$PW_{12}O_{40}]\cdot xH_2O$ (981, 1079, 890 and 799 cm^{-1} for $\nu(W–O_t)$, $\nu(P–O_a)$, $\nu(W–O_b)$ and $\nu(W–O_c)$)[29], both $\nu(P–O_a)$ and $\nu(W–$

O_c) absorption bands in **1** respectively split into two absorption bands primarily because the lower symmetry of the $[\alpha\text{-}PW_{11}O_{39}]^{7-}$ fragments in **1** is lower than that of the $[\alpha\text{-}PW_{12}O_{40}]^{3-}$ polyoxoanion[12]. The absorption bands at 3137 and 2961 cm^{-1} are indicative of the stretching vibrations of -NH_2 and -CH_2 groups on dap ligands whereas the bending vibration bands of -NH_2 and -CH_2 groups are respectively seen at 1583 and 1453 cm^{-1}. The broad absorption band centered at 3463 cm^{-1} implies the presence of lattice or coordinate water molecules.

3. 3 Thermal analysis

In order to probe the thermogravimetric (TG) process of **1**, the TG analysis of **1** has been carried out in flowing air atmosphere with a heating rate of 10 $^oC\ min^{-1}$ in 25～1000 ^oC (Fig. 6). The TG curve exhibits a two-step weight loss procedure with a total weight loss of 18.57% between 25 and 1000 ^oC (calcd. 18.05%). The first-step weight loss of 1.72% from 25 to 298 ^oC is assigned to the release of four water molecules of crystallization and one coordinate water molecule (calcd. 1.33%). After then, the second weight loss of 16.85% is approximately attributed to the sublimation of one P_2O_5 together with the removal of eleven dap ligands and eleven oxygen atoms (calcd. 16.72%). Actually, such phenomenon that some oxygen atoms will lose during the course of decomposing the W-O skeleton has been previously encountered[30]. The experimental values are in good agreement with the theoretical values.

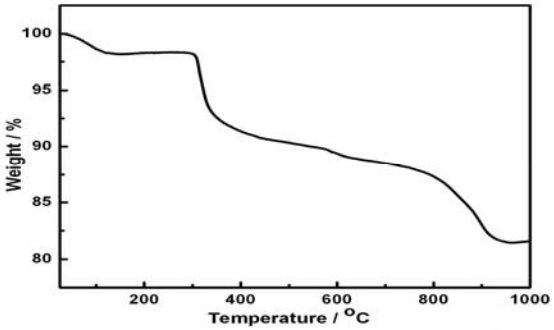

Fig. 6. TG curve of 1 measured in flowing N_2 atmosphere at a heating rate of 10 $^oC\ min^{-1}$ in the 25～1000 ^oC range

REFERENCES

(1) Zheng, S. T.; Zhang, J.; Clemente-Juan, J. M.; Yuan, D. Q.; Yang, G. Y. Poly(polyoxotungstate)s with 20 nickel centers: from nanoclusters to one-dimensional chains. *Angew. Chem. Int. Ed.* **2009**, 48, 7176−7179.

(2) Han, Q. X.; He, C.; Zhao, M.; Qi, B.; Niu, J. Y.; Duan, C. Y. Engineering chiral polyoxometalate hybrid metal−organic frameworks for asymmetric dihydroxylation of olefins. *J. Am. Chem. Soc.* **2013**, 135, 10186−10189.

(3) Zhou, J.; Zhao, J. W.; Wei, Q.; Zhang, J.; Yang, G.Y. Two tetra-Cd^{II}-substituted vanadogermanate frameworks. *J. Am. Chem. Soc.* **2014**, 136, 5065−5071.

(4) Zeng, M. H.; Wang, Q. X.; Tan, Y. X.; Hu, S.; Zhao, H. X.; Long, L. S.; Kurmoo, M. Rigid pillars and double walls in a porous metal-organic framework: single-crystal to single-crystal, controlled uptake and release of iodine and electrical conductivity. *J. Am. Chem. Soc.* **2010**, 132, 2561–2563.

(5) Felices, L. S.; Vitoria, P.; Gutiérrez-Zorrilla, J. M.; Lezama, L.; Reinoso, S. Hybrid inorganic-metalorganic compounds containing copper(II)-monosubstituted Keggin polyanions and polymeric copper(I) complexes. *Inorg. Chem.* **2006**, 45, 7748–7757.

(6) Zheng, S. T.; Zhang, J.; Li, X. X.; Fang, W. H.; Yang, G. Y. Cubic polyoxometalate-organic molecular cage. *J. Am. Chem. Soc.* **2010**, **132**, 15102–15103.

(7) Belai, N.; Pope, M. T. Chelated heteroatoms in polyoxometalates and the topological equivalence of $\{Co^{III}(en)\}$ to type II cis-dioxometal centers. Synthesis and structure of $[\{Co(en)(\mu\text{-}OH)_2Co(en)\}\{PW_{10}O_{37}Co(en)\}_2]^{8-}$ and $[K\subset\{Co(en)WO_4\}\{WO(H_2O)\}(PW_9O_{34})_2]^{12-}$. *Chem. Commun.* **2005**, 5760–5762.

(8) Luan, G.; Li, Y.; Wang, S.; Wang, E.; Han, Z.; Hu, C.; Hu, N.; Jia, H. A new α-Keggin type polyoxometalate coordinated to four silver complex moieties: $\{PW_9V_3O_{40}[Ag(2,2'\text{-bipy})]_2[Ag_2(2,2'\text{-bipy})_3]_2\}$. *Dalton Trans.* **2003**, 32, 233–235.

(9) Zhang, S. W.; Wang, Y.; Zhao, J. W.; Ma, P. T.; Wang, J. P.; Niu, J. Y. Two types of oxalate-bridging rare-earth-substituted Keggin-type

phosphotungstates $\{[(\alpha\text{-}PW_{11}O_{39})RE(H_2O)]_2(C_2O_4)\}^{10-}$ and $\{(\alpha\text{-}x\text{-}PW_{10}O_{38})RE_2(C_2O_4)(H_2O)_2\}^{3-}$. *Dalton Trans.* **2012**, 41, 3764–3772.

(10) Niu, J. Y.; Wang, K. H.; Chen, H. N.; Zhao, J. W.; Ma, P. T.; Wang, J. P.; Li, M. X.; Bai, Y.; Dang, D. B. Assembly chemistry between lanthanide cations and monovacant Keggin polyoxotungstates: two types of lanthanide substituted phosphotungstates $[\{(\alpha\text{-}PW_{11}O_{39}H)Ln(H_2O)_3\}_2]^{6-}$ and $[\{(\alpha\text{-}PW_{11}O_{39})Ln(H_2O)(\eta^2,\mu\text{-}1,1)\text{-}CH_3COO\}_2]^{10-}$. *Cryst. Growth Des.* **2009**, 9, 4362–4372.

(11) Pichon, C.; Dolbecq, A.; Mialane, P.; Marrot, J.; Rivière, E.; Sécheresse, F. Square versus tetrahedral iron clusters with polyoxometalate ligands. *Dalton Trans.* **2008**, 37, 71–76.

(12) Cao, J.; Liu, S.; Cao, R.; Xie, L.; Ren, Y.; Gao, C.; Xu, Lin. Organic–inorganic hybrids assembled by bis(undecatungstophosphate) lanthanates and dinuclear copper(II)–oxalate complexes. *Dalton Tra*ns. **2008**, 37, 115–120

(13) Niu, J. Y.; Zhang, S. W.; Chen, H. N.; Zhao, J. W.; Ma, P. T.; Wang, J. P. 1-D, 2-D, and 3-D organic-inorganic hybrids assembled from Keggin-type polyoxometalates and 3d-4f heterometals. *Cryst. Growth Des*. **2011**, 11, 3769–3777.

(14) Zhao, H. Y.; Zhao, J. W.; Yang, B. F.; He, H.; Yang, G. Y. Novel organic-inorganic hybrid one-dimensional chain assembled by oxalate-bridging terbium-substituted phosphotungstate dimers and dinuclear copper(II)-oxalate clusters. *CrystEngComm* **2013**, 15, 5209–5213.

(15) Zhao, H. Y.; Zhao, J. W.; Yang, B.-F.; He, H.; Yang, G. Y. Organic-inorganic hybrids based on monovacant Keggin-type polyoxotungstates and 3d–4f heterometals. *CrystEngComm* **2013**, 15, 8186–8194.

(16) Shi, D. Y.; Zhao, J. W.; Chen, L. J.; Ma, P. T.; Wang, J. P.; Niu, J. Y. Four types of 1D or 2D organic-inorganic hybrids assembled by arsenotungstates and Cu^{II}–$Ln^{III/IV}$ heterometals. *CrystEngComm* **2012**, 14, 3108–3119.

(17) Zhao, J. W.; Shi, D. Y.; Chen, L. J.; Ma, P. T.; Wang, J. P.; Zhang, J.; Niu, J. Y. Tetrahedral polyoxometalate nanoclusters with tetrameric rare-earth cores and germanotungstate vertexes. *Cryst. Growth Des.* **2013**, 13, 4368−4377.

(18) Zhao, J. W.; Li, Y. Z; Ji, F.; Yuan, J.; Chen, L. J.; Yang, G. Y. Syntheses, structures and electrochemical properties of a class of 1-D double chain polyoxotungstate hybrids $[H_2dap][Cu(dap)_2]_{0.5}[Cu(dap)_2(H_2O)][Ln(H_2O)_3(\alpha\text{-}GeW_{11}O_{39})]\cdot 3H_2O$. *Dalton Trans*. **2014**, 43, 5694–5706.

(19) Zhao, J. W.; Cao, J.; Li, Y. Z.; Zhang, J.; Chen, L. J. First tungstoantimonate-based transition-metal−lanthanide heterometallic hybrids functionalized by amino acid ligands. *Cryst. Growth Des*. **2014**, 14, 6217–6229.

(20) Domaille, P. J.; Hervé, G.; Tézé, A. Vanadium(V) substituted dodecatungstophosphates. *Inorg. Synth.* 1990, 27, 96–104.

(21) Sheldrick, G M. *SHELXS 97, Program for Crystal Structure Solution,* University of Göttingen: Göttingen, Germany, **1997**.

(22) Sheldrick, G. M. *SHELXL97, Program for Crystal Structure Refinement,* University of Göttingen: Göttingen, Germany, **1997**.

(23) Peacock, R. D.; Weakley, T. J. R. Heteropolytungstate complexes of the lanthanide elements. Part I. Preparation and reactions. *J. Chem. Soc. A* **1971**, 1836–1839.

(24) Peacock, R. D.; Weakley, T. J. R. Heteropolytungstate complexes of the lanthanide elements. Part II. Electronic spectra: a metal–ligand charge-transfer transition of cerium(III). *J. Chem. Soc. A* **1971**, 1937–1940.

(25) Gaunt, A. J.; May, I.; Sarsfield, M. J.; Collison, D.; Helliwell, M.; Denniss, I. S. A rare structural characterisation of the phosphomolybdate lacunary anion, $[PMo_{11}O_{39}]^{7-}$. Crystal structures of the Ln(III) complexes, $(NH_4)_{11}[Ln(PMo_{11}O_{39})_2]\cdot 16H_2O$ (Ln = Ce^{III}, Sm^{III}, Dy^{III} or Lu^{III}). *Dalton Trans.* **2003**, 32, 2767–2771.

(26) Copping, R.; Gaunt, A. J.; May, I.; Sarsfield, M. J.; Collison, D.; Helliwell, M.; Dennissc, I.S.; Apperley, D. C. Trivalent lanthanide lacunary phosphomolybdate complexes: a structural and spectroscopic study across the series $[Ln(PMo_{11}O_{39})_2]^{11-}$. *Dalton Trans.* **2005**, 34, 1256–1262.

(27) Moulton, B.; Abourahma, H.; Bradner, M. W.; Lu, J. J.; McManus, G.. J.; Zaworotko, M. J. *Chem. Commun.* **2003**, 1342–1343.

(28) Luo, J.; Leng, C. L; Chen, L. J.; Yuan, J.; Li, H. Y.; Zhao, J. W. Three 3D organic–inorganic hybrid heterometallic polyoxotungstates assembled from 1:2-type $[Ln(\alpha\text{-}SiW_{11}O_{39})_2]^{13-}$ silicotungstates and $[Cu(dap)_2]^{2+}$ linkers. *Synth. Met.* **2012**, 162, 1558–1565.

(29) Shi, D. Y.; Chen, L. J.; Zhao, J. W.; Wang, Y.; Ma, P. T.; Niu, J. Y. Two novel 2D organic–inorganic hybrid lacunary Keggin phosphotungstate 3d–4f heterometallic derivatives: $[Cu(en)_2]_2H_6[Ce(\alpha\text{-}PW_{11}O_{39})_2]\cdot 8H_2O$ and $[Cu(dap)_2(H_2O)][Cu(dap)_2]_{4.5}[Dy(\alpha\text{-}PW_{11}O_{39})_2]\cdot 4H_2O$. *Inorg. Chem. Commun.* **2011**, 14, 324–329.

(30) Reinoso, S.; Dickman, M. H.; Kortz, U. A novel hexatungstate fragment stabilized by dimethyltin groups: $[\{(CH_3)_2Sn\}_2(W_6O_{22})]^{4-}$. *Inorg. Chem.* **2006**, 45, 10422−10424.